Nonlinear interaction of intense laser pulses and an inhomogeneous electron-positron-ion plasma

Li-Hong Cheng, Rong-An Tang, Ai-Xia Zhang, and Ju-Kui Xue*
College of Physics and Electronics Engineering, Northwest Normal University, Lanzhou 730070, China
(Received 22 October 2012; revised manuscript received 6 January 2013; published 28 February 2013)

The nonlinear interaction of an ultraintense short laser beam and an inhomogeneous electron-positron-ion (EPI) plasma is investigated. It is found that the presence of positrons and inhomogeneity results in strong modulational and filamentational instabilities, which induce strong nonlinear interactions between the laser beam and the inhomogeneous EPI plasma. Light beam focusing, filamentation, trapping, and nonlinear interaction between the trapped light spots and the inhomogeneous plasma are observed. Interestingly, we find that the inhomogeneity of the plasma can not only boost a mechanism for light beam self-focusing and filamentation but also provide an effective way to localize and trap the beam in the region one wanted.

DOI: 10.1103/PhysRevE.87.025101 PACS number(s): 52.35.Mw, 52.27.Ep

The nonlinear interaction between an ultraintense short laser beam and plasma is of great interest in various fundamental research and technological applications [1–3]. These include relativistic optical guiding, harmonic excitation, wakefield generation, laser pulse frequency shifting, pulse compression, and particle acceleration. Especially, the nonlinear dynamics of intense laser pulses in electron-positron-ion (EPI) plasma have receive a great deal of attention [4–10]. Light beam compression, focusing, and trapping in self-created density holes, light beam filamentation, stable localized solutions, and self-modulational instability in EPI plasmas are discussed. In fact, propagation of an intense short laser beam in plasma can also lead to pair production, resulting in a three-component EPI plasma [4,11,12]. Abundant production of electron-positron (EP) pairs in the collision of a multipetawatt laser beam and a solid target is predicated, and the result shows that the positron density can be up to 10^{26} m^{-3} [13,14]. Recently, EP plasma has been produced in a laboratory by irradiating a solid gold target with an intense picosecond laser pulse [15–17]. The results show that the positron density can be up to 10^{16} cm^{-3}. The results also predict that, with the increasing performance of high-energy ultrashort laser pulses, a high-density (up to 10^{18} cm^{-3}) relativistic pair plasma is achievable. Thus, from these theoretical and experimental investigations we can expect that the investigation of nonlinear interaction of a pair plasma and high-intensity electromagnetic fields is significant for future high-intensity laser experiments. However, the previous investigations about the propagation of a laser beam in EPI plasma were mainly limited to homogeneous cases. In fact, up to now, few investigations have been devoted to the effect of plasma inhomogeneity on pulse propagation [18–25]. It was shown that axial [18–21] or radial [23–25] inhomogeneity can further boost the self-focusing and compression mechanism and localize the pulse intensity compared with a homogeneous plasma.

In this Brief Report, taking into account the effects of equilibrium density inhomogeneity and positron concentration, we study the nonlinear propagation of the intense laser pulses in an inhomogeneous EPI plasma. Starting from the Maxwell equations and Poisson's equation, we show that the system of governing equations can be reduced to a modified nonlinear Schrödinger equation (NLSE) with a density inhomogeneity effect. Linear, Gaussian, and cosine density inhomogeneities along the axial direction are discussed. It is shown that the presence of positrons and inhomogeneity results in strong modulational and filamentational instabilities, which induce strong nonlinear interaction between the laser beam and the inhomogeneous EPI plasma. Rich and interesting phenomena are observed. We find that the inhomogeneity can not only boost a mechanism for light beam self-focusing and filamentation but also provide an effective way to localize and trap the pulse in the region we wanted.

We investigate the propagation of intense laser pluses in a smooth inhomogeneous EPI plasma. We assume that the electron and the positron densities are homogenous in the radial r direction but inhomogeneous in the axial z direction. The local equilibrium state of the three-component system is characterized by the dimensionless local charge neutrality,

$$n_{e0}(z) = \alpha n_{p0}(z) + (1-\alpha) n_{i0}(z), \tag{1}$$

where $n_{e0}(z)$, $n_{p0}(z)$, and $n_{i0}(z)$ are the unperturbed number densities of the electrons, positrons, and ions, respectively. The coefficient $\alpha = n_{p0}(0)/n_{e0}(0)$ denotes the ratio of positron density to the electron density at $z = 0$. The electrons and positrons are denoted by the subscripts e and p, respectively. The ions do not respond to the dynamics under consideration and provide a neutralizing background due to their relatively large inertia.

In order to describe the nonlinear propagation of intense light in such a plasma, we start with the Maxwell equations. The wave equation (in the Coulomb gauge $\nabla \cdot \boldsymbol{A} = 0$) and the Poisson equation of the system take the forms [1,5,7]

$$\frac{\partial^2 \boldsymbol{A}}{\partial t^2} - \nabla^2 \boldsymbol{A} = \alpha n_p \boldsymbol{v}_p - n_e \boldsymbol{v}_e \tag{2}$$

and

$$\nabla^2 \varphi = n_e - \alpha n_p - (1-\alpha) n_{i0}(z). \tag{3}$$

Here $\boldsymbol{A}$ and φ are the vector and scalar potentials, respectively, n_e (n_p) is the electron (positron) number density, and $\boldsymbol{v}_e$ ($\boldsymbol{v}_p$) is the electron (positron) velocity in the electromagnetic fields. The system is closed by invoking the equation of

*Corresponding author: xuejk@nwnu.edu.cn

motion,

$$\frac{\partial \boldsymbol{p}_{e,p}}{\partial t} + (\boldsymbol{v}_{e,p}\cdot\nabla)\boldsymbol{p}_{e,p} = \mp\left[-\nabla\varphi - \frac{\partial \boldsymbol{A}}{\partial t} + \boldsymbol{v}_{e,p}\times(\nabla\times\boldsymbol{A})\right] - \frac{T_{e,p}}{n_{e,p}}\nabla n_{e,p}, \tag{4}$$

for each of the mobile components. Here $\boldsymbol{p}_e$ ($\boldsymbol{p}_p$) is the electron (positron) momentum, and T_e (T_p) is the electron (positron) temperature. Equations (1)–(4) are dimensionless, with the following scalings:

$$t \sim \omega_e t, \quad \boldsymbol{r} \sim \frac{\omega_e}{c}\boldsymbol{r}, \quad \boldsymbol{v}_{e,p} \sim \frac{\boldsymbol{v}_{e,p}}{c}, \quad \boldsymbol{p}_{e,p} \sim \frac{\boldsymbol{p}_{e,p}}{m_0 c}, \quad T_{e,p} \sim \frac{T_{e,p}}{m_0 c^2}, \quad n_{i0}(z) \sim \frac{n_{i0}(z)}{n_{i0}(0)}, \quad n_{e,p} \sim \frac{n_{e,p}}{n_{e0,p0}(0)}, \quad \hat{A} \sim \frac{e}{m_0 c^2}\hat{A}, \tag{5}$$

where $\hat{A} \equiv [\boldsymbol{A};\varphi]$, $\omega_e = [4\pi e^2 n_{e0}(0)/m_0]^{1/2}$ is the electron plasma frequency, e is the magnitude of the electron charge, and m_0 is the rest mass of electrons.

For the propagation of a circularly polarized electromagnetic wave with a frequency ω_0 and wave number $\boldsymbol{k}(\boldsymbol{r}) = k(z)\hat{\boldsymbol{z}}$ along the axial direction, the vector potential can be represented as

$$\boldsymbol{A} = \frac{1}{2}a(\boldsymbol{r},t)(\hat{\boldsymbol{x}} + \mathrm{i}\,\hat{\boldsymbol{y}})\exp\left(i\int \boldsymbol{k}(\boldsymbol{r})\cdot d\boldsymbol{r} - \mathrm{i}\omega_0 t\right) + \text{c.c.} \tag{6}$$

Since the dimensionless quiver velocity is given by $\boldsymbol{v}_{e,p} = \boldsymbol{p}_{e,p}/\gamma_{e,p}$, where $\gamma_{e,p} = (1 + \boldsymbol{p}_{e,p}^2)^{1/2}$, Eq. (4) in the transverse direction is satisfied by [1]

$$\boldsymbol{p}_{e,p} = \pm\boldsymbol{A} \tag{7}$$

and

$$\nabla[\pm\varphi - \gamma_{e,p} - T_{e,p}\ln n_{e,p}] = 0. \tag{8}$$

It is noted that Eq. (7) governs the high-frequency response of the electrons and the positrons with the same frequency ω_0 as that of the incident waves, and $a(\boldsymbol{r},t)$ is slowly varying along the spatial $\boldsymbol{r}$ and time t. From Eq. (7), the electron and positron velocities are

$$\boldsymbol{v}_e = \frac{\boldsymbol{A}}{\gamma}, \quad \boldsymbol{v}_p = -\frac{\boldsymbol{A}}{\gamma}, \tag{9}$$

where $\gamma = (1 + |\boldsymbol{A}|^2)^{1/2} \equiv \gamma_{e,p}$. Equation (8) describes the electron and positron low-frequency response (neglecting the electron inertia for slow motion). The second term in Eq. (8) is the usual expression for the relativistic ponderomotive force. The expressions for the electron and positron number densities can be obtained by integrating Eq. (8):

$$n_e = n_{e0}(z)\exp\left[-\frac{\gamma - 1}{T_e} + \frac{\varphi}{T_e}\right], \tag{10a}$$

$$n_p = n_{p0}(z)\exp\left[-\frac{\gamma - 1}{T_p} - \frac{\varphi}{T_p}\right]. \tag{10b}$$

Using Eq. (9), Eq. (2) becomes

$$\frac{\partial^2 \boldsymbol{A}}{\partial t^2} - \nabla^2\boldsymbol{A} + \frac{\alpha n_p + n_e}{\sqrt{1 + |\boldsymbol{A}|^2}}\boldsymbol{A} = 0. \tag{11}$$

Substituting Eq. (6) and the dispersion relation $\omega_0^2 - k^2 = \alpha n_{p0}(z) + n_{e0}(z)$ into Eq. (11), we obtain

$$i\omega_0\frac{\partial a}{\partial t} + i(\boldsymbol{k}\cdot\nabla)a + \frac{1}{2}\nabla^2 a + \frac{\alpha n_{p0}(z) + n_{e0}(z)}{2}a - \frac{1}{2}\frac{\alpha n_p + n_e}{\sqrt{1 + |a|^2}}a = 0. \tag{12}$$

Noting that all terms in this dynamic vary on a slow time scale, it is now convenient to induce new variables, $t = \tau\omega_0$ and $\boldsymbol{r} = \boldsymbol{r}' + \boldsymbol{v}_g\tau\omega_0$, and denote $\boldsymbol{v}_g = \boldsymbol{k}/\omega_0$ as the group velocity of light. Thus, Eq. (12) takes the form

$$i\frac{\partial a}{\partial \tau} + \frac{1}{2}\nabla^2 a + \frac{\alpha n_{p0}(z) + n_{e0}(z)}{2}a - \frac{1}{2}\frac{\alpha n_p + n_e}{\sqrt{1 + |a|^2}}a = 0. \tag{13}$$

For convenience, r' in Eq. (13) is still expressed by r. We assume that the unperturbed electrons and positrons obey the same distribution in the axial direction, viz., $n_{e0}(z) = n_{p0}(z) = n_0(z)$. From Eqs. (1), (10), and (3) we have

$$\varphi = (1 - \sqrt{1 + a^2})(\alpha\beta_p - \beta_e)/(\alpha\beta_p + \beta_e), \tag{14}$$

where $\beta_e = 1/T_e$, $\beta_p = 1/T_p$. Then, Eq. (13) takes the form

$$i\frac{\partial a}{\partial \tau} + \frac{1}{2}\nabla^2 a + \left\{\frac{\alpha + 1}{2} - \frac{\alpha\exp[\beta(1 - \sqrt{1 + |a|^2})]}{2\sqrt{1 + |a|^2}} - \frac{\exp[\alpha\beta(1 - \sqrt{1 + |a|^2})]}{2\sqrt{1 + |a|^2}}\right\}n_0(z)a = 0, \tag{15}$$

where $\beta = 2\alpha\beta_p\beta_e/(\alpha\beta_p + \beta_e)$ denotes the temperature parameter. The plasma inhomogeneity is expressed by the term $n_0(z)$. When $n_0(z) = 1$, the system is reduced to the homogeneous case.

The modulational instability of an arbitrary large amplitude electromagnetic pump wave governed by Eq. (15) can be investigated by standard techniques. Accordingly, we let $a = (a_0 + a_1)\exp(i\delta\tau)$, where a_0 is a real constant, a_1 ($\ll a_0$) denotes the amplitude of the perturbation, and δ is the nonlinear frequency shift caused by the nonlinear interaction. Then, for a smooth inhomogeneous plasma (i.e., $n_0(z)$ is slowly varying along the axial z), the nonlinear frequency shift δ can be obtained from Eq. (15):

$$\delta = \left\{\frac{\alpha + 1}{2} - \frac{\alpha\exp\left[\beta\left(1 - \sqrt{1 + a_0^2}\right)\right]}{2\sqrt{1 + a_0^2}} - \frac{\exp\left[\alpha\beta\left(1 - \sqrt{1 + a_0^2}\right)\right]}{2\sqrt{1 + a_0^2}}\right\}n_0(z). \tag{16}$$

Letting $a_1 = (X + iY)\exp[i\int \boldsymbol{K}(\boldsymbol{r})\cdot d\boldsymbol{r} - i\Omega\tau]$, where X and Y are real constants and $\Omega(\boldsymbol{K})$ is the frequency (wave vector) of the low-frequency modulations, and linearizing Eq. (15) with

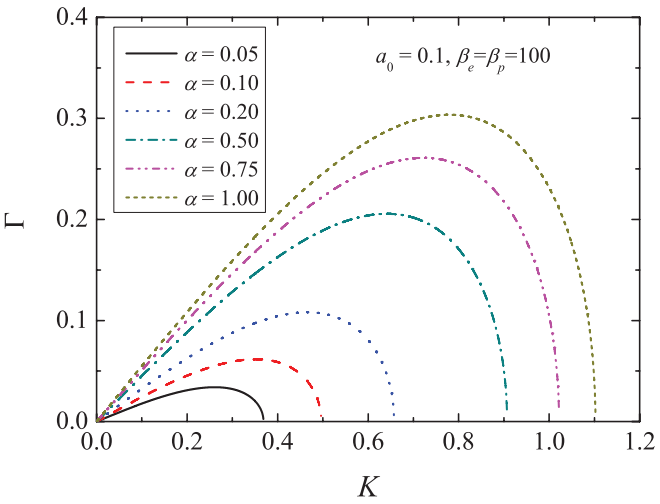

FIG. 1. (Color online) The modulational instability growth rate Γ vs the wave number K for different values of the positron-to-electron density ratio α.

respect to X and Y, we obtain the modulational instability growth rate $\Gamma = -i\Omega$:

$$\Gamma = \frac{K}{\sqrt{2}}\left(\left\{\alpha\left(1+\beta\sqrt{1+a_0^2}\right)\exp\left[\beta\left(1-\sqrt{1+a_0^2}\right)\right]\right.\right.$$
$$\left.+\left(1+\alpha\beta\sqrt{1+a_0^2}\right)\exp\left[\alpha\beta\left(1-\sqrt{1+a_0^2}\right)\right]\right\}$$
$$\left.\times\frac{a_0^2}{2\left(1+a_0^2\right)^{\frac{3}{2}}}n_0(z)-\frac{K^2}{2}\right)^{\frac{1}{2}}. \qquad (17)$$

where $K = |\boldsymbol{K}|$. In Fig. 1, we show the growth rate Γ as a function of K for the positron-to-electron density ratio $\alpha = 0.05, 0.10, 0.20, 0.50, 0.75$, and 1.00 in the homogeneous case, i.e., with $n_0(z) = 1$ in terms of Eq. (17). The plasma parameters are $a_0 = 0.1$, $\beta_e = \beta_p = 100$. We see that the growth rate increases with α. In pure EP plasma ($\alpha = 1$) we obtain the largest instability increment, and the modulational instability reaches a maximum due to the largest positron concentration. On the other hand, the presence of positrons has a strong effect on modulational instability. When the positrons are absent ($\alpha = 0$), the system is stable. The phenomenon can be understood in terms of the ponderomotive force, which appears because of the interaction between the high-frequency laser wave and the background plasma. The force acting on particles is directed along the decrease of the laser field energy density and does not depend on the sign of the electric charge of particles. Its magnitude is proportional to the gradient of the intensity of the laser and is inversely proportional to the plasma particles' mass. Because of the large ion mass, the ponderomotive forces acting on ions are much smaller compared with the forces acting on electrons and positrons; thus it can be neglected here. If the laser wave amplitude has a maximum at some points, then the ponderomotive force tends to push electrons away from those points and leaves behind an ambipolar field. The ambipolar field prevents the motion of electrons. If the positron presents, positrons are pushed away together with electrons, and the ambipolar field will be decreased. Due to the decreasing of the ambipolar field induced by the increasing positron population, more electrons

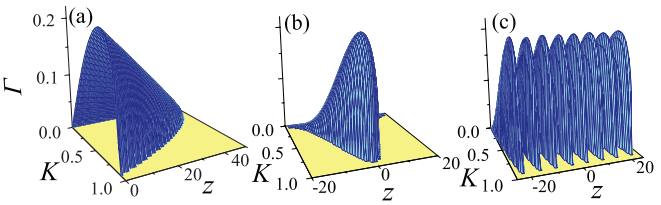

FIG. 2. (Color online) The modulational instability growth rate Γ vs the wave number K and the axial direction z. The initial parameters are $a_0 = 0.1, \beta_e = \beta_p = 100$, $\alpha = 0.5$. (a) $n_0(z) = 1 + bz$, $b = -0.02$; (b) $n_0(z) = \exp(-z^2/L_z), L_z = 16\pi$; (c) $n_0(z) = 0.5(1 - \cos z)$.

will be expulsed away by the ponderomotive force, and then the modulational instability of the system can be enhanced.

In Fig. 2, we show the growth rate Γ as a function of K and the light propagation direction z for the inhomogeneous cases with $\alpha = 0.5$ in terms of Eq. (17). In order to investigate the effects of electron and positron distribution on the modulational instability, three types of inhomogeneous cases are discussed: a slow variation of the electron and positron density along axial direction $n_0(z) = 1 + bz$, where b is a characteristic inhomogeneity parameter [Fig. 2(a)]; a Gaussian density distribution $n_0(z) = \exp(-z^2/L_z)$, $L_z = 16\pi$, where L_z is the simulation box length [Fig. 2 (b)]; and a cosine distribution $n_0(z) = 1/2(1 - \cos z)$ [Fig. 2(c)]. It is clear that the inhomogeneity has a strong influence on modulational instability. The higher the density is, the stronger the modulational instability becomes. Figures 1 and 2 indicate that the interaction between the laser beam and the inhomogeneity of EPI plasma would induce rich and interesting phenomena.

In order to investigate the effects of positron concentration and the inhomogeneity on the propagation of large amplitude electromagnetic beams, we assume axial symmetry around the z direction and solve Eq. (15) numerically for the time evolution of the amplitude of vector potential. As an initial condition, we take a modulated beam of the form $a = 0.1[1 + 0.02\sin(2\pi z/L_z) + 0.02\cos(4\pi z/L_z) +$

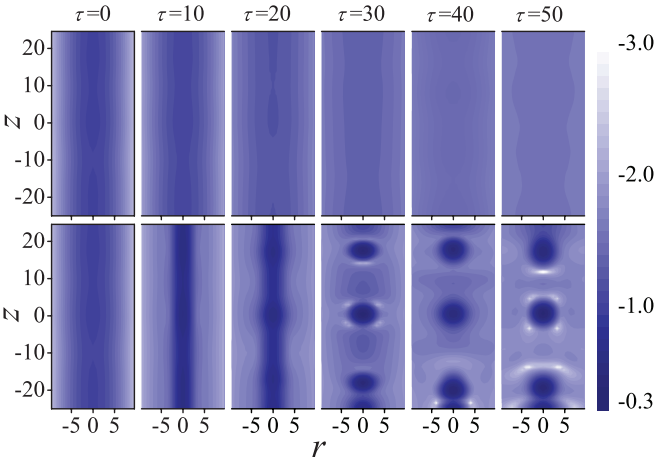

FIG. 3. (Color online) The light amplitude a in $\log_{10}$ scale at six different times τ for the homogeneous case. The horizontal axis represents the distribution along the radial (r) coordinate, and the axial (z) distribution is on the vertical axis. The top row is for $\alpha = 0$, the bottom row is for $\alpha = 0.5$.

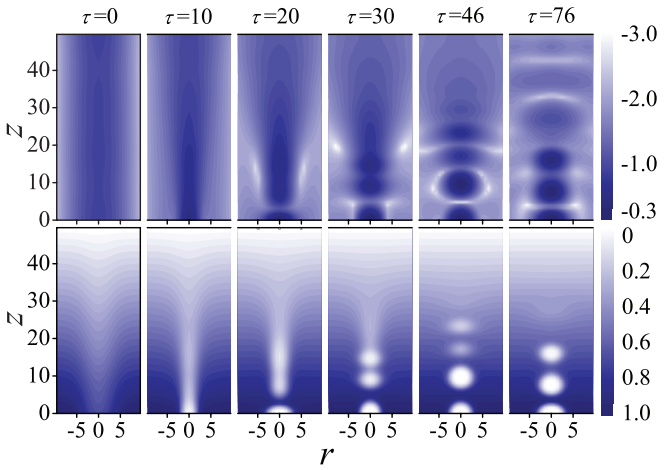

FIG. 4. (Color online) (top) The light amplitude a and (bottom) the normalized electron number density as functions of r and z at six different times τ for $n_0(z) = 1 + bz$, $b = -0.02$, $\alpha = 0.5$.

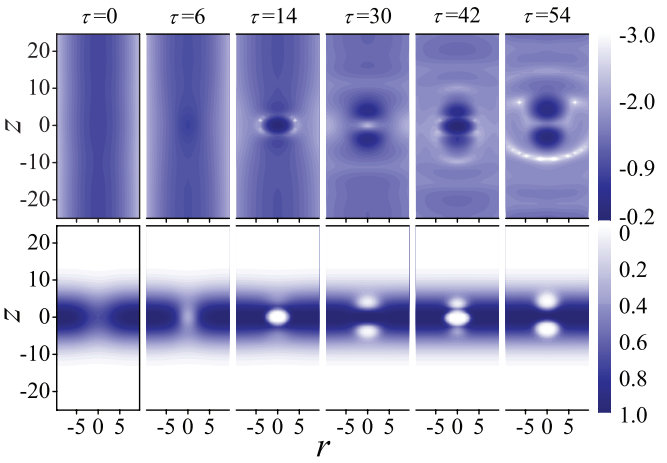

FIG. 6. (Color online) (top) The light amplitude a in $\log_{10}$ scale and (bottom) the normalized electron number density as functions of r and z at six different times τ for $n_0(z) = \exp(-z^2/L_z)$, $\alpha = 0.5$.

$0.02\cos(6\pi z/L_z)]\exp(-r^2/32)$, where L_z is the simulation box length and r is the radial space coordinate.

Figure 3 shows the time evolution of the light amplitude a for the cases without (the top row, $\alpha = 0$) and with (the bottom row, $\alpha = 0.5$) positrons in homogeneous plasma. It is clear that, when the positrons are absent, the light beam cannot be localized and is finally defocused. However, when the positrons are present, the light beam first self-focuses and then breaks up into localized filaments due to modulational instability.

Figures 4–7 show the numerical simulations of time evolution of a and n_e for inhomogeneous cases. For a linear axial density distribution $n_0(z) = 1 + bz$ (see Fig. 4), the self-focusing and the localization of the light and the creation of electron density holes (where the light is trapped) take place in the region with high density ($z \lesssim 30$), where modulational instability is stronger [see Fig. 2(a)]. For the Gaussian (Figs. 5 and 6) and cosine (Fig. 7) types of density distribution, however, the self-focusing and the light localization and the creation of electron density holes only present at the highest-density regions, where modulational instability is strongest [see Figs. 2(b) and 2(c)]. Interestingly, for the Gaussian density distribution with the larger positron proportion ($\alpha = 0.5$; Fig. 6), the localized light spots experience a process of breaking up into two pieces and merging into one spot alternately. For the cosine density distribution (Fig. 7), merging of the periodically localized eight light spots occurs; correspondingly, the electron density holes trapping the light also exhibit the same process. These phenomena indicate that a strong nonlinear interaction between light and an inhomogeneous plasma can exist.

To summarize, the nonlinear propagation of arbitrary large amplitude light pulses in an inhomogeneous EPI plasma is studied. We find that the positron concentration and plasma inhomogeneity have a strong influence on the modulational and filamentational instabilities in EPI plasma. Light beam focusing and trapping in self-created density holes induced by modulational and filamentational instabilities depend on the

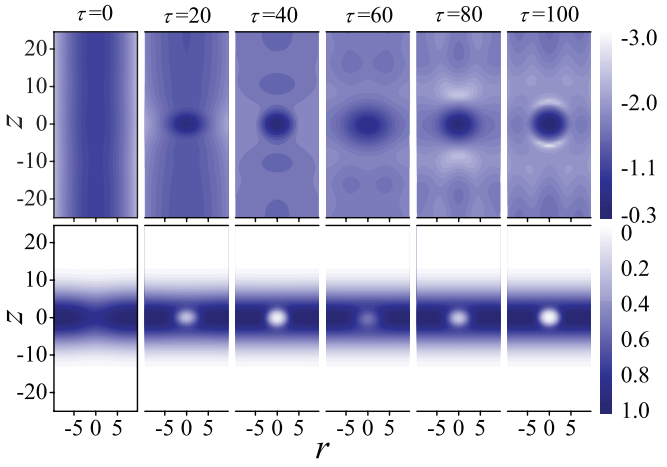

FIG. 5. (Color online) (top) The light amplitude a in $\log_{10}$ scale and (bottom) the normalized electron number density as functions of r and z at six different times τ for $n_0(z) = \exp(-z^2/L_z)$, $L_z = 16\pi$, $\alpha = 0.2$.

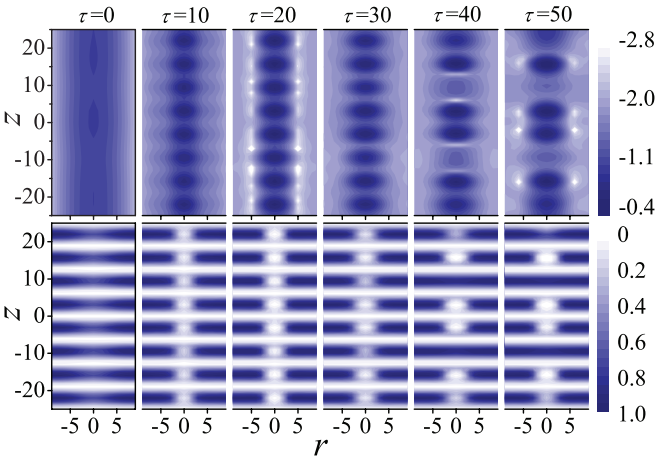

FIG. 7. (Color online) (top) The light amplitude a in $\log_{10}$ scale and (bottom) the normalized electron number density as functions of r and z at six different times τ for $n_0(z) = 0.5(1 - \cos z)$, $\alpha = 0.5$.

inhomogeneous nature. The light beam localization occurs at the highest-density regions, where the modulational instability is strong. On the other hand, the inhomogeneity of the plasma can not only boost a mechanism for light beam self-focusing and filamentation but also provide an effective way to localize and trap the pulse in the region we wanted. The present results should be useful in understanding the dynamics of intense laser pulses in EPI plasma.

Acknowledgments. This work is supported by the National Natural Science Foundation of China under Grants No. 10975114 and No. 11274255, by the Natural Science Foundation of Gansu province under Grant No. 2011GS04358, and by the Natural Science Foundation of Northwest Normal University under Grants No. NWNU-KJCXGC-03-48, No. NWNU-LKQN-10-27, and No. NWNU-LKQN-12-12.

[1] P. K. Shukla, N. N. Rao, M. Y. Yu, and N. L. Tsintsadze, Phys. Rep. **138**, 1 (1986).
[2] D. Umstadter, J. Phys. D **36**, R151 (2003).
[3] E. Esarey, C. B. Schroeder, and W. P. Leemans, Rev. Mod. Phys. **81**, 1229 (2009).
[4] V. I. Berezhiani, D. D. Tskhakaya, and P. K. Shukla, Phys. Rev. A **46**, 6608 (1992).
[5] V. I. Berezhiani and S. M. Mahajan, Phys. Rev. Lett. **73**, 1110 (1994).
[6] V. I. Berezhiani and S. M. Mahajan, Phys. Rev. E **52**, 1968 (1995).
[7] P. K. Shukla, M. Marklund, and B. Eliasson, Phys. Lett. A **324**, 139 (2004).
[8] A. Sharma, I. Kourakis, and P. K. Shukla, Phys. Rev. E **82**, 016402 (2010).
[9] G. Lehmann and K. H. Spatschek, Phys. Rev. E **83**, 036401 (2011).
[10] F. A. Asenjo, F. A. Borotto, A. C.-L. Chian, V. Muñoz, J. A. Valdivia, and E. L. Rempel, Phys. Rev. E **85**, 046406 (2012).
[11] C. M. Surko, M. Leventhal, W. S. Crane, A. Passner, and F. Wysocki, Rev. Sci. Instrum. **57**, 1862 (1986).
[12] V. I. Berezhiani, D. P. Garuchava, and P. K. Shukla, Phys. Lett. A **360**, 624 (2007).
[13] E. P. Liang, S. C. Wilks, and M. Tabak, Phys. Rev. Lett. **81**, 4887 (1998).
[14] C. P. Ridgers, C. S. Brady, R. Duclous, J. G. Kirk, K. Bennett, T. D. Arber, A. P. L. Robinson, and A. R. Bell, Phys. Rev. Lett. **108**, 165006 (2012).
[15] H. Chen, S. C. Wilks, J. D. Bonlie, E. P. Liang, J. Myatt, D. F. Price, D. D. Meyerhofer, and P. Beiersdorfer, Phys. Rev. Lett. **102**, 105001 (2009).
[16] H. Chen *et al*., Phys. Rev. Lett. **105**, 015003 (2010).
[17] H. Chen *et al*., High Energy Density Phys. **7**, 225 (2011).
[18] R. K. Khanna and R. C. Chouhan, Nonlinear Opt. (Mclc) B **29**, 61 (2002).
[19] A. Sharma, M. P. Verma, M. S. Sodha, and A. Kumar, J. Plasma Phys. **70**, 163 (2004).
[20] M. Varshney (Asthana), K. A. Qureshi, and D. Varshney, J. Plasma Phys. **72**, 195 (2006).
[21] A. Sharma and I. Kourakis, Plasma Phys. Controlled Fusion **52**, 065002 (2010).
[22] J. Fuchs, E. d'Humières, Y. Sentoku, P. Antici, S. Atzeni, H. Bandulet, S. Depierreux, C. Labaune, and A. Schiavi, Phys. Rev. Lett. **105**, 225001 (2010).
[23] H. S. Brandi, C. Manus, G. Mainfray, and T. Lehner, Phys. Rev. E **47**, 3780 (1993).
[24] P. Jha, A. Malviya, A. K. Upadhyay, and V. Singh, Plasma Phys. Controlled Fusion **50**, 015002 (2008).
[25] M. S. Sodha and M. Faisal, Phys. Plasmas **15**, 033102 (2008).